SPANDIDOS PUBLICATIONS

ONCOLOGY LETTERS 14: 6645-6649, 2017

Multiple pulmonary metastases with halo-sign from malignant mixed Müllerian tumors

HONG-WEI TIAN*, WEI-BING YANG*, MENG-JIE YANG, JING-YUAN LIU, JIAN-CHU ZHANG, XIAO-NAN TAO and QIONG ZHOU

Department of Respiratory and Critical Care Medicine, Union Hospital, Tongji Medical College, Huazhong University of Science and Technology, Wuhan, Hubei 430022, P.R. China

Received January 24, 2016; Accepted June 15, 2017

DOI: 10.3892/ol.2017.7036

Abstract. The lungs are one of the most common organs to which cancer metastasizes, but are a location not common for uterine sarcoma. A malignant mixed Müllerian tumor (MMMT) of the uterus is an extremely rare and aggressive sarcoma, characterized by a mixture of epithelial and mesenchymal components. There are few reports regarding the pulmonary metastasis from MMMTs. The present study presents the case of a 58-year-old woman with hemoptysis and post-menopausal vaginal bleeding. The woman was initially diagnosed with invasive aspergillosis based on a chest computed tomography (CT) scan showing multiple pulmonary nodular opacities surrounded by a ground-glass attenuation halo (halo-sign). Diagnostic curettage and a percutaneous CT-guided lung biopsy were conducted for the pathological diagnosis. Finally, the diagnosis was confirmed as MMMT with lung metastasis based on the histopathological examination of cervical canals, uterus and lung specimens, which showed a mixture of carcinomatous and sarcomatous elements, and morphology exhibiting hyperchromatic nuclei and necrosis. Immunohistochemical staining was positive for vimentin, focally positive for p16, and negative for napsin, cytokeratin 7 (CK7), CK20, carcinoembryonic antigen, carbohydrate antigen 125, homeobox protein CDX2 and villin in the lung specimens. This case highlights that pulmonary metastatic tumor from uterine sarcoma can present as halo-sign, which is commonly observed in pulmonary aspergillosis. Therefore, it needs to be considered in the differential diagnosis of such lesions, and pathological confirmation is required.

Correspondence to: Dr Qiong Zhou, Department of Respiratory and Critical Care Medicine, Union Hospital, Tongji Medical College, Huazhong University of Science and Technology, 1277 Jiefang Avenue, Wuhan, Hubei 430022, P.R. China
E-mail: zhouqiongtj@126.com

*Contributed equally

Abbreviations: MMMTs, malignant mixed Müllerian tumors; CT, computed tomography

Key words: pulmonary metastases, halo-sign, uterine sarcoma, hemoptysis, malignant mixed Müllerian tumors

Introduction

Malignant mixed mullerian tumors (MMMTs) are uncommon and lethal neoplasms. They occur in postmenopausal females and comprise only 1-2% of uterine cancer and 3-5% of all uterine malignancies (1). Clinical presentation usually consists of abdominal pain, distension and atypical bleeding. Though common in the uterus, these tumors may also arise epithelial (carcinoma) and mesenchymal (sarcoma) elements (1).

Two of the organs most frequently affected by cancer metastasis are the lungs, and at some stage, ~30% of all cancer patients will develop lung metastases (2). This is mainly as the lung is the first filter in the general circulation (3,4). Secondly, the low pressure system and slow blood flow velocities of the pulmonary circulation are apt to allow tumor cells to stagnate (3,4). Metastatic neoplasm often present as multiple lung nodules and masses when incidental can be detected by a diagnostic chest radiography of computed tomography (CT) scan (5). Metastatic lung cancer frequently has non-specific symptoms and CT scans reveal single or multiple spherical nodules with a smooth periphery (5). However, metastatic lung cancer presenting with sustained hemoptysis as the initial symptom, with multiple nodular opacities surrounded by a ground-glass attenuation halo (halo-sign), which are commonly observed in pulmonary aspergillosis (6), have not been reported before.

The present study reports a case of MMMTs with lung metastasis in a patient who intially presented with multiple pulmonary nodular opacities surrounded by a ground-glass attenuation halo, mimicking invasive aspergillosis.

Case report

A 58-year-old woman was referred to the Department of Respiratory and Critical Care Medicine (Union Hospital, Tongji Medical College, Huazhong University of Science and Technology, Wuhan, Hubei, China) with hemoptysis and post-menopausal vaginal bleeding on January 10th, 2015. At 4 months prior to this admission, the patient presented with hemoptysis, or bloody sputum, after a rough cough. The patient

reported no fever, night sweats or chest pain. At 1 month prior to the present admission, the patient presented with vaginal bleeding, ~5 ml every day, without cervical pain. The patient was initially treated with empiric antibiotics for presumptive pneumonia in local hospital. Short-term follow-up revealed that the hemoptysis and vaginal bleeding of the patient had progressively worsened over time, thus the patient was admitted to our hospital for further evaluation.

A chest examination was normal. No detectable peripheral lymphadenopathy was found. Laboratory results included the following: normal creatinine, blood urea nitrogen and serum electrolyte levels; aminotransferase, 8 U/l (5-35 U/l); aspartate aminotransferase, 12 U/l (8-40 U/l); albumin, 37.2 g/l (35-55 g/l); total protein, 61.0 g/l (64-83 g/l); leukocyte count, $4.87x10^9$/l ($3.5\text{-}5.5x10^9$/l); red blood cell count, $3.27x10^{12}$/($3.8\text{-}5.1x10^{12}$/l); hemoglobin, 79 g/l (110-150 g/l); and platelet count, $281x10^9$/l ($125\text{-}350x10^9$/l). Serum test results were negative for carcinoembryonic antigen (CEA), carbohydrate antigen (CA125), hepatitis B virus, human immunodeficiency virus, hepatitis C virus, 1-3-β glucan antigen-D, galactomannan antigen, tuberculosis antibody, immunoglobulin E and procalcitonin. Additionally, a serum test showed an erythrocyte sedimentation rate of 36 mm/h (<20 mm/h) and a C-reactive protein level of 3.48 mg/l (0-8 mg/l). Sputum smear and cultures were negative for bacteria, fungus and *Mycobacterium tuberculosis*. Other results were as follows: Urinary occult blood test, 3+; and urinary red blood cell quantification, 194.0/μl (<25/μl).

Chest CT revealed multiple nodular opacities surrounded by a ground-glass attenuation halo (halo-sign) in the peripheral regions of the bilateral lung field. The majority of the lesions reached underneath the pleura, interstitial shadows such as ground-glass-like shadows and thickening of the interlobular walls were observed, and a small amount of bilateral pleural effusion existed (Fig. 1).

A whole-body fluorine-18 fluorodeoxyglucose positron emission tomography (^{18}F-FDG-PET) scan revealed mild ^{18}F-FDG uptake in several nodular lesions in the lung; the maximum standand uptake value (SUVmax) was within the range of 2.0-10.4 (normal value, <2.5). Furthermore, highly abnormal accumulation was found in a number of bone lesions, including those of the collarbone, ribs, femur and pelvis; the SUVmax was within the range of 4.5-11.2, demonstrating multiple bony metastases. However, no definite FDG uptake was found in the cervix and uterus, which may have been diminished due to the diagnostic curettage of the cervix and endometrium performed prior to the PET scan (Fig. 2).

Bronchoscopic examination revealed only a small volume of fresh blood in the right main bronchus. The washing fluid from the alveoli was a reddish color and a cytological smear test showed some epithelial cells, lymphocytes, granulocytes and a small amount of other cells.

Uterine ultrasound showed a postmenopausal uterus with endometrial hyperplasia. The initial cytological diagnosis of the Pap smear was of cervical adenocarcinoma (data not shown). Subsequently, biopsies of the cervix and endometrium were performed via diagnostic curettage. The cervical biopsy at the 3, 6, 9 and 12 o'clock positions of the endometrium revealed chronic cervicitis associated with coating squamous epithelial hyperplasia and focally squamous metaplasia of the cervical gland (data not shown). The genetic detection of human papillomavirus via the cervical swab was negative.

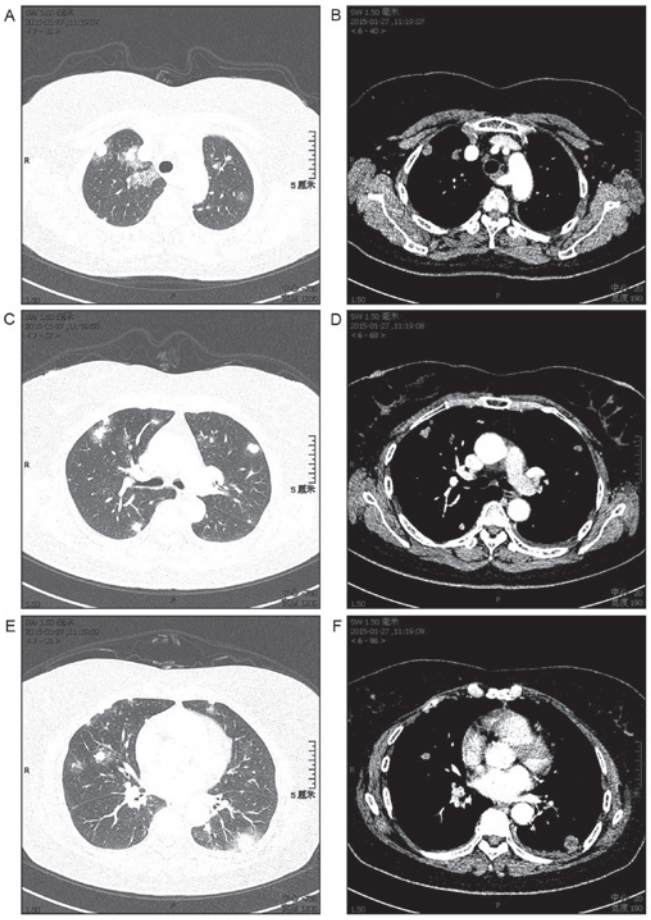

Figure 1. Chest CT scans of the patient. Chest CT showing multiple nodular opacities surrounded by a ground-glass attenuation halo (halo-sign) in the bilateral lung. CT image of (A) the upper lobe in the parenchymal window and (B) the mediastinal window. CT image of (C) the upper lobe and the apical lower lobe in the parenchymal and (D) mediastinal window. CT image of the middle and lower lobe in (E) the parenchymal window and (F) the mediastinal window. CT, computed tomography.

Cervical canals and uterus biopsies were fixed in 10% formalin for 6 h at 37˚C, embedded with paraffin, cut into 5 μm section and stained with hematoxylin-eosin for 20 min at room temperature. Finally, slides were viewed using an imaging microscope (magnification, x100, Olympus BX51; Olympus, Tokyo, Japan). The cells were observed to exhibit spindle nuclei, nuclear pleomorphism, partial necrosis and scanty indistinct cytoplasm, and the tissues showed biphasic tumors with epithelial and mesenchymal components, which was consisitent with an MMMT (Fig. 3).

Percutaneous lung sampling by CT-guided biopsy was conducted for the pathological diagnosis. Histological examination of the lung biopsy sample revealed an infiltrating tumor of predominantly sarcoma morphology composed of multiple atypical spindle cells with hyperchromatic nuclei and multinucleation, and partial necrosis (Fig. 4). Serial sections of the lung specimen were used for immunohistochemical analysis. Primary antibodies used for staining were anti-human-vimetin mAb (cat. no. LAB040Hu71; Biocompare, San Antonio, TX, USA), anti-human-p16 (cat. no. MBS9386591; MyBioSource,

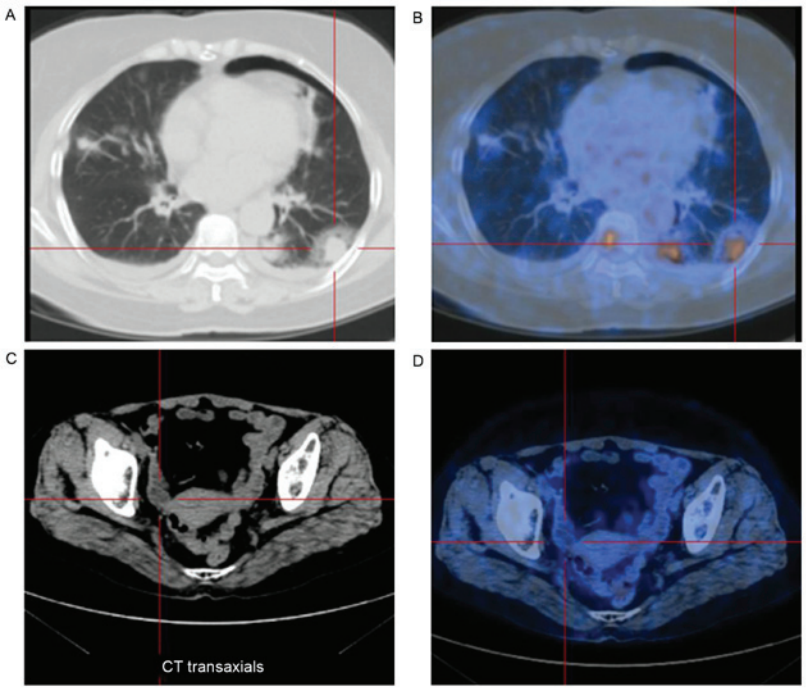

Figure 2. (A) CT image showing a nodular opacity surrounded by a ground-glass attenuation halo in the lower lobe of the lung. (B) FDG PET/CT images showing increased FDG activity in the area of nodular opacity, with a maximum standardized uptake value of 2.0-10.4. (C) CT image showing the uterus with thickened endometrium, and no definite nodules in the cervix and uterus. (D) FDG PET/CT showing no definite fluorodeoxyglucose uptake in the cervix and uterus. CT, computed tomography; FDG, fluorodeoxyglucose; PET, positron emission tomography.

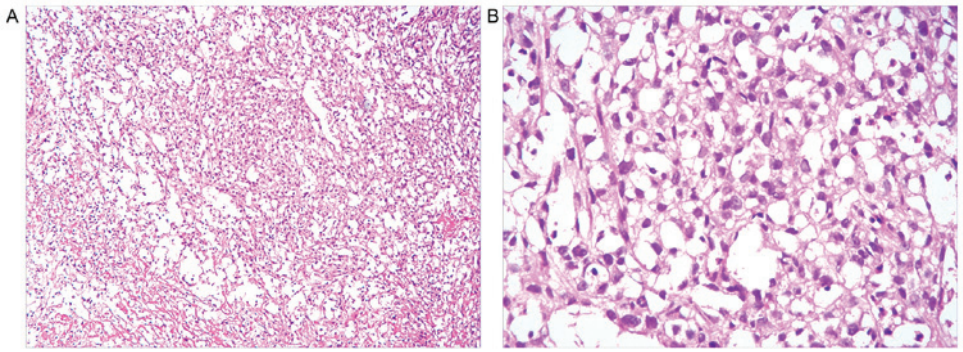

Figure 3. Hispathological examination of the endometrial biopsies following diagnostic curettage showing cells with spindle nuclei, nuclear pleomorphism, partial necrosis and scanty to indistinct cytoplasm, which was consisitent with a malignant mixed Müllerian tumor. (A) Magnification, x100 and (B) x400. Hematoxylin and eosin staining.

San Diego, CA, USA), anti-human-napsin (cat. no. ab73021; Abcam, Cambrige, UK), anti-human-cytokeratin 7 (CK7) (cat. no. ZA103; Zomanbio, Beijing, China), anti-human-CK20 (cat. no. ab76126; Abcam), anti-human-CEA (cat. no. ab133633; Abcam), anti-human CA125 (cat. no. 119-13259; RayBiotech Inc., Atlanta, GA, USA), anti-human-CDX2 (cat. no. MAB3665; R&D Systems, Minneapolis, MN, USA), and anti-human-villin (cat. no. sc-58897; Santa Cruz Biotechnology, Inc., Santa Cruz, CA, USA), all diluted to 1:100. Secondary antibodies used for staining included horseradish peroxidase (HRP)-conjugated goat anti-mouse immunoglobulin G (IgG) (cat. no. 31430) or HRP-conjugated goat anti-rabbit IgG antibodies (cat. no. 31460; Thermo Fisher Scientific, Inc.). Slides were de-waxed with xylene and rehydrated using a graded ethanol series (100, 95, 80, 70 and 50%) into water. For antigen retrieval, sections were heated in citrate buffer (pH 6.0) for 10 min at 95˚C in a microwave oven. After cooling to room temperature, the sections were digested with 0.05% trypsin for 10 min at 37˚C. Endogenous peroxidase activity was quenched using 0.3% H_2O_2 in methanol for 30 min at room temperature. Following PBS washes, non-specific antibody binding was blocked by incubating slides with 10% normal goat non-immune serum (cat. no. 50062Z; Invitrogen; Thermo Fisher Scientific, Inc.) at 37˚C for 30 min. Subsequent to washing with PBS, sections were incubated with primary antibodies at 4˚C overnight with 1:100 diluitions. Following further PBS washes, sections were incubated with the secondary antibodies (1:100) for 30 min at room temperature. Finally, after incubating with diamino-benzidine for 30 min at room temperature, slides revealed immunoreactivity for vimentin, and were focally positive for p16 and negative for napsin, CK7, CK20, CEA, CA125, homeobox protein CDX2 and villin (Fig. 5).

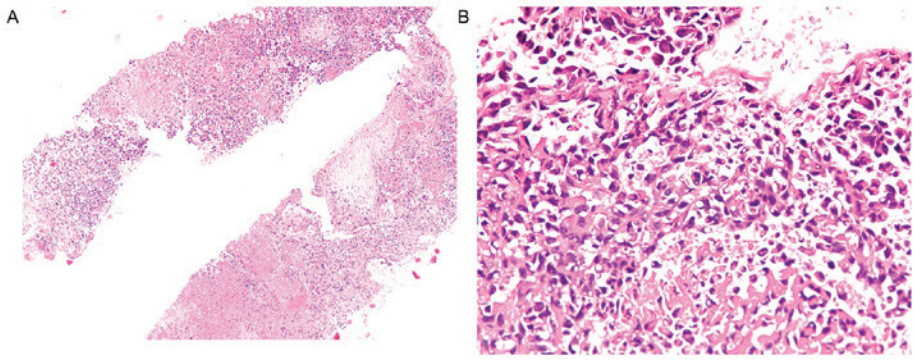

Figure 4. Histological examination of the lung biopsy sample revealing an infiltrating tumor of predominantly sarcoma morphology composed of a large quantity of atypical spindle cells with hyperchromatic nuclei and multinucleation, and partial necrosis. (A) Magnification, x40 and (B) x200. Hematoxylin and eosin staining.

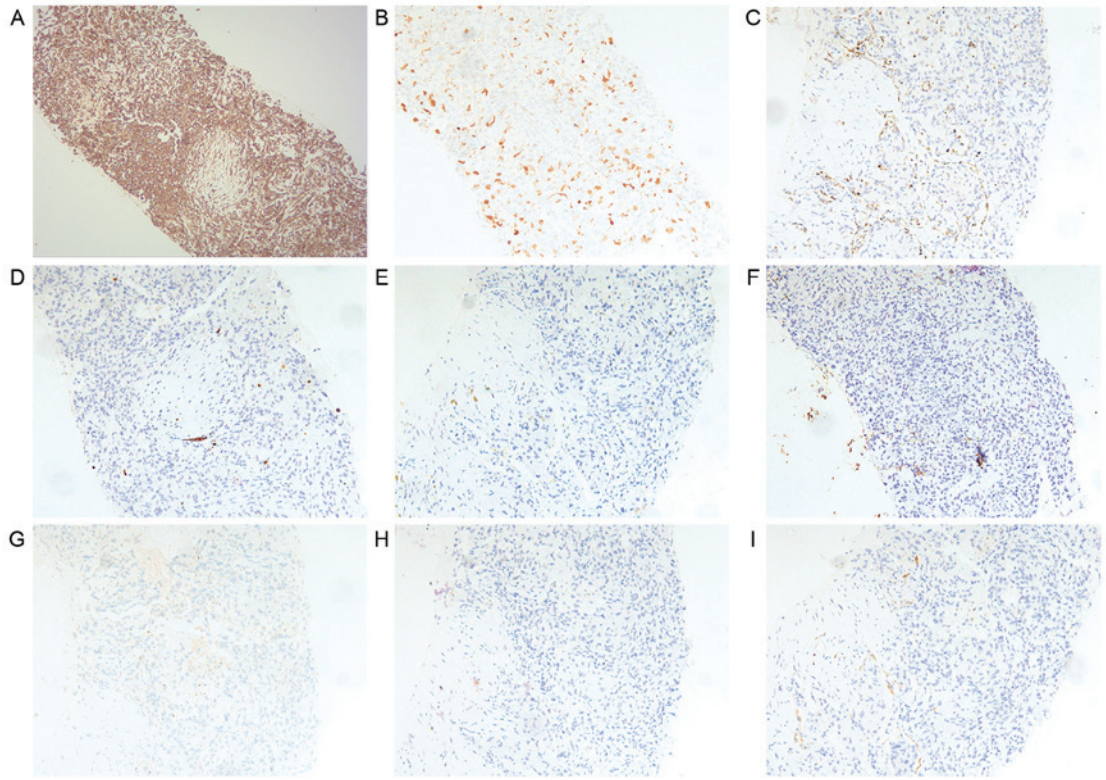

Figure 5. Hispathological examination of the pulmonary lesion sampled by percutaneous computed tomography-guided lung biopsy. Immunohistochemical staining of the lung specimen revealing (A) immunoreativity for vimentin (original magnification, x100), (B) focal positivity for p16 (original magnification, x100) and negative results for (C) napsin, (D) CK7, (E) CK20, (F) carcinoembryonic antigen, (G) carbohydrate antigen 125, (H) homeobox protein CDX2 and (I) villin. Original magnification, x100. CK, cytokeratin.

Histopathological examination of specimens from the uterus, cervix and lung nodular tissues showed the same features as each other. These immunohistochemical features, particularly vimentin positivity, were identical to the findings of tissues originating from the uterus. Based on these histopathological and immunohistochemical findings, the diagnosis of MMMT with pulmonary metastasis was confirmed.

The patient's treatment was initiated by administration of intravenous voriconazole at a dose of 200 mg twice a day for 7 days. However, the state of the lung field was not improved and was aggravated further, we discontinued anti-fungi therapy and performed serial examinations mentioned above. Unfortunately, the patient ended treatment and was discharged due to financial difficulties. She had a highly aggressive course of disease and died only 4 months after diagnosis.

Written informed consent was obtained from the patient for publication of the present study.

Discussion

MMMTs, also known as carcinosarcomas, are composed of malignant epithelial and mesenchymal elements (carcinomatous and sarcomatous components), and have an estimated incidence of <2 cases/100,000 women per year (7,8). MMMTs can also originate in the vagina, ovary, uterine cervix or female peritoneum, but these forms are even rarer (9-12). The clinical

initial presentation of MMMTs has been recorded as pain and abdominal expansion in 62.5% of cases, and as a palpable mass and vaginal bleeding in 25% of cases (13).

Although the most common site of distant metastasis is the lungs (14), uterine cancer metastasis to the lungs is rare (5.41%); according to the Chinese Academy of Medical Sciences Cancer Hospital analysis of patients admitted over a period of 10 years (1999-2009), ~3569 (40%) cancer patients developed lung metastases. Metastasis to the lungs is usually found through routine examinations, including lung CT and whole body PET. Patients with metastatic lung cancer present with primary tumor-related complications as the main clinical symptom and have no clear lung-related symptoms at an early stage (5). In the present case, hemoptysis that was reported as the only early clinical symptoms, and followed by vaginal bleeding are rare.

CT scans of metastatic lung cancer frequently reveal single or multiple spherical nodules with a smooth periphery (5). In the present case, CT revealed the characteristic halo sign, a solid nodule surrounded by a ground-glass attenuation halo. In patients suffering from immunosuppression, the halo sign is highly indicative of an angioinvasive fungal infection, most typically aspergillosis (15). Other infections, including mycobacterial and certain viral infections, also present with the halo sign on CT (16). In the present study, the female patient was initially suspected of having pulmonary invasive aspergillosis due to the typical halo-sign of the pulmonary lesion, however, β-D-glucan and galactomannan tests were negative. The radiology findings demonstrated well demarcated nodules without marked lymph node enlargement in the mediastinum and hilum (17,18). Accounting for these features, a metastatic lung tumor of extrathoracic origin was also a possible diagnosis. Finally, the nodular opacities surrounded by a ground-glass attenuation halo (halo-sign) in this case were presumed to be due to the proliferation of metastatic lung tumor cells, followed by the destruction of peripheral vessels, which accounted for the continuous hemoptysis (19).

In conclusion, cases with lung metastases from MMMTs with sustained hemoptysis as the initial only symptom, and multiple nodular opacities surrounded by a ground-glass attenuation halo (halo-sign) are rare. Physician must be aware of metastatic pulmonary tumors that closely resemble aspergillomas infection and show hemoptysis as the initial symptom, not only when considering infectious diseases, but also in oncological practice.

Acknowledgements

The authors would like to thank Dr Li Peng (Department of Pathology, Union Hospital) for performing and assisting with the hispathological examination. This study was supported by grants from the National Natural Science Foundation of China (nos. 81470274 and 81770090) and the 12th Five-Year National Science and Technology Program of Social Development, Ministry of Science and Technology, China (no. 2012BAI05B02).

References

1. Bhoil A, Kashyap R, Bhattacharya A and Mittal BR: F-18 fluorodeoxyglucose positron emission tomography/computed tomography in a rare case of recurrent malignant mixed mullerian tumor. World J Nucl Med 13: 64-66, 2014.
2. Davidson RS, Nwogu CE, Brentjens MJ and Anderson TM: The surgical management of pulmonary metastasis: Current concepts. Surg Oncol 10: 35-42, 2001.
3. Suresh K and Shimoda LA: Lung Circulation. Compr Physiol 6: 897-943, 2016.
4. Al-Mehdi AB, Tozawa K, Fisher AB, Shientag L, Lee A and Muschel RJ: Intravascular origin of metastasis from the proliferation of endothelium-attached tumor cells: A new model for metastasis. Nat Med 6: 100-102, 2000.
5. Margaritora S, Porziella V, D'Andrilli A, Cesario A, Galetta D, Macis G and Granone P: Pulmonary metastases: Can accurate radiological evaluation avoid thoracotomic approach? Eur J Cardiothorac Surg 21: 1111-1114, 2002.
6. Greene RE, Schlamm HT, Oestmann JW, Stark P, Durand C, Lortholary O, Wingard JR, Herbrecht R, Ribaud P, Patterson TF, *et al*: Imaging findings in acute invasive pulmonary aspergillosis: Clinical significance of the halo sign. Clin Infect Dis 44: 373-379, 2007.
7. Kanthan R and Senger JL: Uterine carcinosarcomas (malignant mixed müllerian tumours): A review with special emphasis on the controversies in management. Obstet Gynecol Int 2011: 470795, 2011.
8. D'Angelo E and Prat J: Pathology of mixed Müllerian tumours. Best Pract Res Clin Obstet Gynaecol 25: 705-718, 2011.
9. Ahuja A, Safaya R, Prakash G, Kumar L and Shukla NK: Primary mixed mullerian tumor of the vagina-a case report with review of the literature. Pathol Res Pract 207: 253-255, 2011.
10. McCluggage WG: Mullerian adenosarcoma of the female genital tract. Adv Anat Pathol 17: 122-129, 2010.
11. Lee SH, Kim J, Kim JH, Lee KH, Park JS and Hur SY: Malignant mixed mullerian tumor of the cervix including components of a rhabdomyosarcoma: Case report and literature review. Eur J Gynaecol Oncol 31: 462-466, 2010.
12. Kuyumcuoğlu U and Kale A: Homologous type of malignant mixed Mullerian tumor of the uterus presenting as a cervical mass. J Chin Med Assoc 72: 533-535, 2009.
13. Montalvo-Esquivel G, Chanona-Vilchis JG, Herrera-Gómez A, Meneses-García AA and Isla-Ortiz D: Primary ovarian carcinosarcoma. Report of eight cases. Ginecol Obstet Mex 82: 483-489, 2014 (In Spanish).
14. Spanos WJ Jr, Peters LJ and Oswald MJ: Oswald Patterns of recurrence in malignant mixed müllerian tumors of the uterus. Cancer 57: 155-159, 1986.
15. Greene RE, Schlamm HT, Oestmann JW, Stark P, Durand C, Lortholary O, Wingard JR, Herbrecht R, Ribaud P, Patterson TF, *et al*: Imaging findings in acute invasive pulmonary aspergillosis: Clinical significance of the halo sign. Clin Infect Dis 44: 373-379, 2007.
16. Lee YR, Choi YW, Lee KJ, Jeon SC, Park CK and Heo JN: CT halo sign: The spectrum of pulmonary diseases. Br J Radiol 78: 862-865, 2005.
17. Internullo E, Cassivi SD, Van Raemdonck D, Friedel G and Treasure T; ESTS Pulmonary Metastasectomy Working Group: Pulmonary metastasectomy: A survey of current practice amongst members of the European Society of Thoracic Surgeons. J Thorac Oncol 3: 1257-1266, 2008.
18. Saito Y, Omiya H, Kohno K, Kobayashi T, Itoi K, Teramachi M, Sasaki M, Suzuki H, Takao H and Nakade M: Pulmonary metastasectomy for 165 patients with colorectal carcinoma: A prognostic assessment. J Thorac Cardiovasc Surg 124: 1007-1013, 2002.
19. Kim Y, Lee KS, Jung KJ, Han J, Kim JS and Suh JS: Halo sign on high resolution CT: Findings in spectrum of pulmonary diseases with pathologic correlation. J Comput Assist Tomogr 23: 622-626, 1999.